

Research paper

Comparative Analysis of the Standards ANSI/IEEE C.37 and 141 and IEC 60909 for Short-Circuit Calculation in Industrial Systems

Análisis comparativo de las normas ANSI/IEEE C.37 y 141 e IEC 60909 para el cálculo de cortocircuitos en sistemas industriales

[John Muñoz-Goez](#)¹, [Joseph C. Sosapanta-Salas](#)¹, and [Jhon Noguera-Jiménez](#)²

¹Institución Universitaria Pascual Bravo, Medellín, Colombia. ² Unidad Central del Valle del Cauca, Tuluá, Colombia.

Correspondence E-mail: j.sosapantasa@pascualbravo.edu.co

Received: July 22nd, 2024

Modified: December 28th, 2025

Accepted: February 23rd, 2026

Abstract

Context: Calculating short-circuit currents is key to equipment sizing and protection coordination in electrical power systems. However, methodological differences between ANSI/IEEE C.37 and 141 and IEC 60909 create uncertainty when selecting the most appropriate approach. This study addresses this problem through a comparative analysis based on computer simulations that evaluate both methodologies under equivalent conditions.

Method: An industrial system with 44 busbars is modeled in ETAP (version 20.0), considering grid connection, local generation, and rotating loads. Short-circuit currents are calculated while following the procedures of both standards, and five representative fault points are analyzed. The evaluation includes six parameters: symmetrical inrush current, half-cycle closing current, peak fault current, interrupting current, asymmetrical breaking current, and steady-state current.

Results: The IEC method yields values between 5 and 10% higher than those obtained with ANSI/IEEE in most cases. The greatest differences are observed at busbars near generators and higher-power rotating machines, reaching up to 9.34% in the inrush current. These variations are mainly associated with the treatment of the X/R ratio and the voltage factor c applied in IEC.

Conclusions: The IEC 60909 standard offers more conservative estimates for demanding designs, while ANSI/IEEE is useful in preliminary analyses, providing practical criteria for selecting the standard based on system criticality.

Keywords: electrical system modeling, electrical transient analyzer program (ETAP), load flows, protection coordination

Resumen

Contexto: El cálculo de corrientes de cortocircuito es clave para el dimensionamiento de equipos y la coordinación de protecciones en sistemas eléctricos de potencia. Sin embargo, las diferencias metodológicas entre las normas ANSI/IEEE C.37 y 141 e IEC 60909 generan incertidumbre al seleccionar el enfoque más adecuado. Este estudio aborda esta

problemática mediante un análisis comparativo basado en simulaciones computacionales que evalúan ambas metodologías bajo condiciones equivalentes.

Método: Se modela un sistema industrial de 44 barras en ETAP (versión 20.0), considerando conexión a la red eléctrica, generación local y cargas rotativas. Las corrientes de cortocircuito se calculan siguiendo los procedimientos de ambas normas y se analizan cinco puntos de falla representativos. La evaluación incluye seis parámetros: corriente inicial simétrica, corriente de cierre de medio ciclo, corriente pico de falla, corriente de interrupción, corriente de ruptura asimétrica y corriente en estado estable.

Resultados: El método IEC presenta valores entre un 5 y un 10% superiores a los obtenidos con ANSI/IEEE en la mayoría de los casos. Las mayores diferencias se observan en barras cercanas a generadores y máquinas rotativas de mayor potencia, alcanzando hasta un 9.34 % en la corriente de cierre. Estas variaciones se asocian principalmente con el tratamiento de la relación X/R y el factor de voltaje c aplicado en IEC.

Conclusiones: La norma IEC 60909 ofrece estimaciones más conservadoras para diseños exigentes, mientras que ANSI/IEEE resulta útil en análisis preliminares, proporcionando criterios prácticos para seleccionar la norma según la criticidad del sistema.

Palabras clave: modelado de sistemas eléctricos, programa de analizador de transitorios eléctricos (ETAP), flujos de carga, coordinación de protecciones

I. INTRODUCTION

An accurate calculation of short-circuit currents is essential in ensuring the safety and efficiency of electrical systems, as it directly influences equipment sizing and protection coordination [1]. International guidelines such as the ANSI/IEEE standards (C37.5, C37.13, C37.010, and 141) and IEC 60909 address these calculations. However, they differ in their methodologies and parameters. These discrepancies have generated ongoing debate regarding which standard provides more accurate and suitable results under different system conditions [1], [2], [3]. The literature also highlights that variations in calculated short-circuit currents can affect protection coordination and equipment design, impacting both system safety and operating costs [4].

This study aims to compare the methodologies of both standards by performing short-circuit simulations in an industrial distribution system using the electrical transient analyzer program (ETAP), version 20.0. The analysis will identify key differences between the standards and evaluate their impact on electrical design, providing recommendations to support the selection of the most appropriate standard for specific industrial applications. This comparison is motivated by the need to support engineers in selecting the most suitable standard depending on equipment requirements and study objectives. ANSI/IEEE standards are often preferred for circuit breaker duty and protection coordination studies, while IEC 60909 is commonly applied when standardized calculation assumptions are required.

Several studies and technical standards provide methodologies for calculating short-circuit currents, among which the ANSI/IEEE and IEC approaches stand out. These standards differ significantly in terms of accuracy and applicability, which has motivated a wide range of comparative research, assessing their effectiveness in different contexts. Several comparative studies [4], [5], [6], [7], [8] have conducted detailed evaluations of the IEC 60909 and ANSI/IEEE 141-4 standards, using simulation tools such as DigSILENT PowerFactory to identify key differences in the results yielded by both methods. This complements previous research [9], [10], [11], [12], [13], which has also examined the

accuracy of ANSI and IEC methodologies in industrial environments and highlights their corresponding strengths and limitations. Additionally, subsequent studies [6] have investigated the applicability of IEC-based results in arc-flash calculations according to IEEE 1584, enabling a more comprehensive assessment of the risks associated with electrical faults.

Research focused on 33-11 kV substations [14] has emphasized the importance of selecting an appropriate standard to obtain accurate short-circuit current calculations in complex systems. These studies, along with other analytical works [8], [9], demonstrate the applicability and limitations of each standard across different industrial scenarios. Overall, the reviewed literature highlights the need for further studies that comprehensively assess the differences between ANSI/IEEE and IEC short-circuit calculation approaches. This research aims to contribute to this discussion by providing a comparative analysis that supports engineers in selecting the most suitable standard based on the technical requirements of each system and its specific operating conditions.

This article provides a detailed comparative analysis of the ANSI/IEEE C37 and 141 standards and IEC 60909 for short-circuit current calculations, with a specific focus on identifying discrepancies and similarities in their methodologies and results. Unlike previous studies that focus on a single standard or present non-comparative analyses, this research offers a comprehensive evaluation based on practical case studies and simulations performed using ETAP 20.0. The main technical contributions of this work include the identification of key methodological differences, an assessment of their impact on system safety and reliability, and the development of tools to improve commonly used calculation procedures through the analysis of real-world case studies.

There are methodological and parametric differences between the ANSI/IEEE and IEC standards for calculating short-circuit currents. However, their practical impact on the design and operation of industrial electrical systems has not been sufficiently investigated. Recent updates to both regulations introduce new elements that have not yet been comparatively examined in the existing literature, making it difficult to make an informed selection of the most appropriate approach. This lack of detailed and contextualized analysis creates uncertainty for engineers, particularly regarding the selection of protection devices, equipment settings, and protection coordination, all of which are critical to ensuring the safety and reliability of power systems. This research aims to address this gap by conducting a comparative analysis of both standards, using simulation tools to evaluate and document discrepancies in their results and assess their relevance in specific industrial applications.

This paper is organized as follows. Section II presents a theoretical comparison of short-circuit calculation methods, detailing the technical basis for analyzing alternating-current (AC) and direct-current (DC) components as well as network configuration. Section III describes the methodology, including the data collection process and the general procedure used to compare the standards. Section IV presents the practical case study of an industrial system, including calculations, figures, and results. Section V analyzes the results in terms of the different fault current types and the behavior of the ANSI/IEEE and IEC methods. Finally, Section VI presents the conclusions, and Section VII lists the references consulted for this research.

II. COMPARISON OF SHORT-CIRCUIT METHODS

The following subsections present a general comparison between the ANSI/IEEE C.37, ANSI/IEEE 141, and IEC 60909 standards.

A. General considerations

In ANSI/IEEE standards C37.5, C37.13, C37.010, and 141, short-circuit calculations and equipment impedance values are primarily based on parameters provided by manufacturers, with tolerance margins applied to obtain conservative fault current estimates. As for short-circuit calculations in IEC 60909, a correction factor is applied to synchronous machines and transformers in order to account for nominal operating conditions [15], [16], [17], [18].

B. Pre-fault voltage

The calculated short-circuit currents are proportional to the pre-fault voltages. The ANSI/IEEE standard assumes a maximum operating voltage, typically ranging from 100% to 105% of the nominal system voltage [2]. Therefore, the equivalent source voltage corresponding to the pre-fault condition is computed as follows:

$$U_{pre-fault} = U_{nom} = 1 \text{ p.u.} \quad (1)$$

On the other hand, the IEC standard uses a correction factor c multiplied by the nominal bus voltage and specifies its range for different voltage levels, with 1.1 being the maximum value across all voltage levels. Therefore, the equivalent voltage at the fault location is computed as follows:

$$U_{eq} = c \frac{U_n}{\sqrt{3}} \quad (2)$$

where U_{eq} denotes the equivalent voltage source, U_n is the nominal voltage of the system, and c signifies multiplicative factor.

C. Decay of AC components

ANSI/IEEE favors the adjustment of machine reactance to calculate symmetrical interrupting currents. For induction machines and synchronous motors, the decay of AC short-circuit contributions is modeled using different reactance values for the first cycle and for the system network, spanning 1.5-4 cycles. In the case of synchronous generators, different multipliers are applied to the short-circuit current depending on the electrical distance between the machine and the fault location [15], [19], [20], [21].

In contrast, the IEC recommends considering the proximity of the machine to the short-circuit, the system configuration, and the separation time. For a given fault location, system configuration and source contributions can be classified as *single-supply short-circuits*, *non-meshed network short-circuits*, and *meshed network short-circuits*. When the short-circuit occurs away from the generator, the AC decay is neglected. However, when the short-circuit is close to the generator, the AC decay is calculated based on the interruption time, the machine size, and its short-circuit contribution to the fault [6].

In this study, synchronous motors and induction machines were incorporated by assigning short-circuit current contributions according to their rated capacity and electrical proximity to the faulted bus. The transient decay was modeled using the corresponding sub-transient, transient, and steady-state reactance values, as recommended by each standard, in order to represent the time-dependent reduction of machine contributions during the interruption interval.

D. Decay of DC components

ANSI/IEEE recommends applying multipliers to symmetrical fault currents in order to calculate asymmetrical currents. A key concept in this standard for modeling the decay of DC components is the X/R ratio at the fault location. The standard requires the use of the reactance network to determine the equivalent reactance at the fault point, along with a separate resistance network to calculate the equivalent resistance. In contrast, the IEC standard is not restricted to a single X/R ratio and generally considers more than one. This approach is applicable when the fault is supplied by several independent sources [9], [22], [23], [24].

E. Network configuration

ANSI/IEEE provides a systematic approach for all types of system configurations, whether they be meshed or non-meshed. This simplifies the calculation procedure. IEC offers different approaches to AC and DC decay for single-supply, meshed, and non-meshed systems. This classification refers to a given fault location.

III. METHODOLOGY

An industrial network was modeled while including the necessary elements for a short-circuit study, adjusting the parameters in accordance with the specifications of the studied standards (ANSI/IEEE C.37 and 141 and IEC 60909) [2], [3].

A. Data collection for modeling

The data required to perform a short-circuit study include the following:

- Utility interconnection points and the corresponding fault MVA levels (both three-phase and line-to-ground) to determine the equivalent grid impedance.
- Generation data and rotating load data, including synchronous and induction motors, both individual and aggregated.
- Data for static system equipment, such as transformers, cables, reactors, overhead lines, bus ducts, and other electrical components.
- Impedance values of electrical components.

B. General procedure

The procedure required to determine the short-circuit analysis is illustrated in Fig. 1.

IV. CASE STUDY

The short-circuit study was conducted on a typical 44-bus industrial system to illustrate the required calculations and resulting outcomes. This system, shown in Fig. 2, includes circuits at multiple voltage levels, local generation, a utility interconnection, and a variety of rotating machines. The utility operates at 69 kV, while the plant generators operate at 13.8 kV. Both the utility connection and the generators are assumed to be supplying power, and the rotating loads are considered to be operating near their full capacity. The system includes both induction and synchronous motors, and its general information is shown in Table I [5].

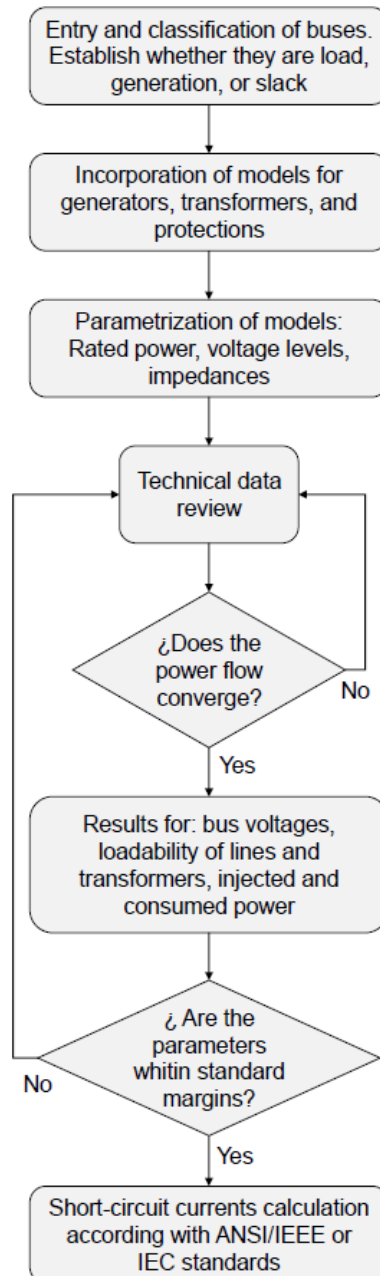


Figure 1. Procedure schematic

Table I
General information

Buses	44
Branches	43
Generators	2
Transmission lines	1
Loads	30
Load-MW	21.766
Load-MVAR	9.009
Generation-MW	21.919
Generation-MVAR	9.969
Losses-MW	0.156
Losses-MVAR	0.961

Considering the network topology and the base study presented in [9], the buses with the highest connected loads and the greatest fault current contributions, according to the short-circuit and load flow simulations, were selected as the fault locations, *i.e.*, 04:MILL-2, 05:FDR F, 10:EMERG, 19:T7SEC, and 50:GEN1.

V. RESULTS ANALYSIS

The following subsections explicitly analyze the differences between the ANSI/IEEE C.37, ANSI/IEEE 141, and IEC 60909 standards. To this effect, the short-circuit modeling parameters, including the fault impedance, source representation, and X/R ratio, are assumed to be identical in order to ensure consistent results.

A. Symmetrical initial short-circuits current

ANSI/IEEE. The RMS (symmetrical) momentary short-circuit current of the first cycle for a zero-impedance fault is calculated as follows:

$$I_{mom,rms,symm} = \frac{U_f}{\sqrt{3}Z_{eq}} \quad (3)$$

where U_f is the pre-fault voltage, and Z_{eq} is the equivalent impedance at faulted bus. The latter is obtained by reducing separate networks for X and R within half-cycle.

IEC. The initial short-circuit current can be calculated using the method of symmetrical components. This approach is applicable to both meshed and non-meshed networks. For faults located close to the generator,

$$I_k'' = \frac{cU_n}{\sqrt{3}Z_k} \quad (4)$$

where Z_k denotes the equivalent impedance at the fault location. For faults far from the generator, impedance correction factors should be considered for generators (K_G) and power plant units (K_S).

The results for the initial symmetrical short-circuit currents are presented in Table II. The discrepancies largely depend on the proximity to the generators. The results show that the IEC short-circuit current values are higher than those obtained using the ANSI/IEEE approach. This difference is mainly attributed to the contribution of rotating machines located along the path between the fault sources and the fault location, which supply the momentary current. In addition, the impedance of the intervening equipment limits the fault current's contribution, affecting the calculated short-circuit currents at specific buses.

Table II
Initial symmetrical short-circuit currents

Bus	V_{nom} [kV]	ANSI/IEEE		IEC			Relative error [%]
		$\frac{X}{R}$	$I_{mom,rms,symm}$ [kA]	Factor c	$\frac{X}{R}$	I_k'' [kA]	
04:MILL-2	13.8	25.169	13.598	1.1	25.2	14.7217	8.27
05:FDR F	13.8	12.439	13.630	1.1	12.5	14.8519	8.96
10:EMERG	13.8	8.881	12.684	1.1	9.0	13.7503	8.40
19:T7SEC	2.4	13.702	18.438	1.1	13.9	20.1240	9.14
50:GEN1	13.8	21.806	13.733	1.1	22.1	14.9371	8.77

B. $\frac{1}{2}$ cycle short-circuit current (closing and blocking)

ANSI/IEEE. The most accurate approach is to use the asymmetrical RMS value of the momentary short-circuit current:

$$I_{mom,rms,asymm} = MF_m \cdot I_{mom,rms,symm} \quad (5)$$

where MF_m denotes the momentary multiplying factor, which is computed as

$$MF_m = \sqrt{1 + 2e^{\frac{-2\pi}{X/R}}} \quad (6)$$

The closing and blocking stress currents are asymmetric fault currents that are calculated in $\frac{1}{2}$ cycle after the start of the fault [5]. ANSI/IEEE recommends the same network because, in $\frac{1}{2}$ cycle, the machine model remains valid. This is performed by applying (6) with a time interval of 0.5 cycles for different X/R values.

IEC. The standard does not explicitly account for asymmetric half-cycle currents. For comparison purposes, these currents were calculated as follows:

$$I_k''_{1/2} = MF_m \cdot I_k'' \quad (7)$$

The results are presented in Table III, considering that the IEC multiplying factor is set nearly identical to that of the methodology given by the ANSI/IEEE, considering the X/R ratio. The resulting short-circuit current values are very similar, with differences of less than 10%,

indicating low discrepancies between the two standards. This outcome is particularly relevant for bus 19:T7SEC, a 2.4 kV node that receives contributions from two high-power motors (1250 and 2500 HP, respectively). These synchronous machines contribute significantly to the initial short-circuit current, leading to very high current values.

Table III
Closing and locking short-circuit currents

Bus	V_{nom} [kV]	ANSI/IEEE		IEC		Relative error [%]
		MF_m	$I_{mom,rms,symm}$ [kA]	MF_m	$I''_{k 1/2}$ [kA]	
04:MILL-2	13.8	1.60	21.75	1.60	23.55	8.28
05:FDR F	13.8	1.49	20.25	1.49	22.08	9.04
10:EMERG	13.8	1.41	17.87	1.41	19.42	8.66
19:T7SEC	2.4	1.50	27.75	1.51	30.34	9.34
50:GEN1	13.8	1.58	21.71	1.58	23.64	8.90

C. Peak fault currents

ANSI/IEEE. The maximum value of the momentary short-circuit current is computed using

$$I_{mom,peak} = MF_p \cdot I_{mom,rms,symm} \quad (8)$$

where MF_p denotes the maximum multiplication factor, which is calculated as follows:

$$MF_p = \sqrt{2} \left(1 + e^{-\frac{\pi}{X/R}} \right) \quad (9)$$

IEC. The recommendation is to perform the calculation separately for each branch of the X/R ratio, and then the maximum current (I_p) is computed as follows:

$$I_p = k\sqrt{2}I''_k \quad (10)$$

where I''_k denotes initial short-circuit current, and k is a factor that depends on the system's X/R ratio at the fault location, which is obtained from Fig. 3.

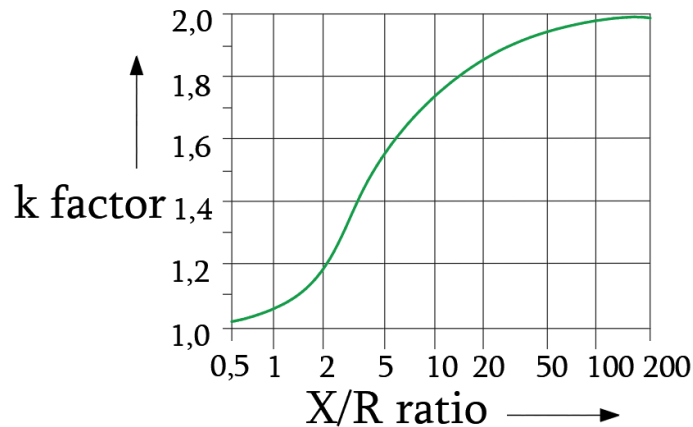


Figure 3. K-factor for series circuits as a function of $\frac{X}{R}$.

These standards describe three techniques for calculating the maximum short-circuit current in meshed networks. The *c* method was selected for this study [1]. Here, the equivalent impedance is calculated at the fault location using a frequency $f_c = 24$ Hz (for a nominal frequency $f = 60$ Hz). The R/X ratio is calculated as follows:

$$\frac{R}{X} = \frac{R_c}{X_c} \cdot \frac{f_c}{f} \quad (11)$$

where R_c is the real equivalent effective resistance component, and X_c denotes the imaginary equivalent effective reactance. The equivalent impedance is given by

$$Z_c = R_c + jX_c \quad (12)$$

The same calculation is applied for faults located either far from or close to the generator. In addition, impedance correction factors for generators (K_G) and/or power plant units (K_S) must be considered [11]. The results are presented in Table IV.

Table IV
Short crest and peak current

Bus	V_{nom} [kV]	ANSI/IEEE		IEC		Relative error [%]
		MF_p	$I_{mon,peak}$ [kA]	Factor k	I_p [kA]	
04:MILL-2	13.8	2.64	35.86	2.6	38.02	6.02
05:FDR F	13.8	2.47	33.65	2.5	36.89	9.64
10:EMERG	13.8	2.35	29.83	2.4	32.61	9.32
19:T7SEC	2.4	2.50	46.05	2.5	49.79	8.13
50:GEN1	13.8	2.61	35.85	2.6	38.03	6.10

D. Breakdown current

ANSI/IEEE. The interrupting currents correspond to the short-circuit currents in the time range of 1.5-4 cycles after fault inception. In this case, the contributions are considered remote, and the calculations are performed based on the total current. The symmetrical value, corrected by the factor MF_r , can be obtained as follows

$$MF_r = \sqrt{1 + 2e^{-\frac{4\pi}{X/R}t}} \quad (13)$$

where t denotes the circuit breaker contact separation time (in cycles). An alternative method is illustrated in Fig 4.

E. Setting the interrupting current

The real multiplication factor (AMF_i) is determined using the *NCAD* relationship.

$$AMF_i = MF_l + NCAD \quad (14)$$

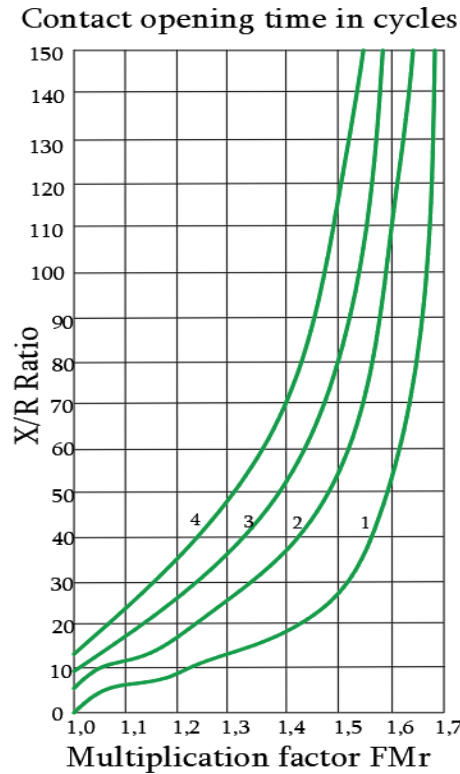


Figure 4. Remote multiplication factor.

For symmetrically rated circuit breakers, the adjusted RMS interrupting short-circuit current is calculated using

$$I_{int,rms,adj} = \frac{AMF_i \cdot I_{int,rms,symm}}{S} \quad (15)$$

where $NCAD$ represents the remote contributions to the total short-circuit current. The variable S is the correction factor that considers the AC high voltage switch.

IEC. The breaking current is used to determine the breaking capacity of automatic switches. For faults located far from the generator, it is expressed as follows:

$$I_b = I''_k \quad (16)$$

For faults near the generator, the DC component of the short-circuit current is given by

$$I_{dc} = I''_k \sqrt{2} e^{\left(\frac{-2\pi f t_{min}}{X/R}\right)} \quad (17)$$

where f is the natural frequency, and t_{min} denotes the minimum response time of the protection device. This standard determines the calculation of the breakdown current by the type of machine [12], [25], [26]. This approach involves the calculation of synchronous machines as given by

$$I_b = \mu \cdot I''_k \quad (18)$$

where μ is decrement factor, I''_k represents the initial short-circuit current, and I_b denotes the symmetrical cutting current. The factor μ is calculated as follows, depending on the minimum delay time, the ratio $\frac{I''_{kG}}{I''_{rG}}$, and the nominal generator current:

$$\begin{aligned}
 \mu &= 0.84 + 0.26 \cdot e^{-0.26 \frac{I''_{kG}}{I''_{rG}}} & t_{min} \\
 &= 0.02s \mu \\
 &= 0.71 + 0.51 \\
 &\cdot e^{-0.30 \frac{I''_{kG}}{I''_{rG}}} & t_{min} \\
 &= 0.05s \mu \\
 &= 0.62 + 0.72 & (19) \\
 &\cdot e^{-0.32 \frac{I''_{kG}}{I''_{rG}}} & t_{min} \\
 &= 0.10s \mu \\
 &= 0.56 + 0.94 \\
 &\cdot e^{-0.38 \frac{I''_{kG}}{I''_{rG}}} & t_{min} \geq 0.25s
 \end{aligned}$$

The factor μ can also be obtained from Fig. 5.

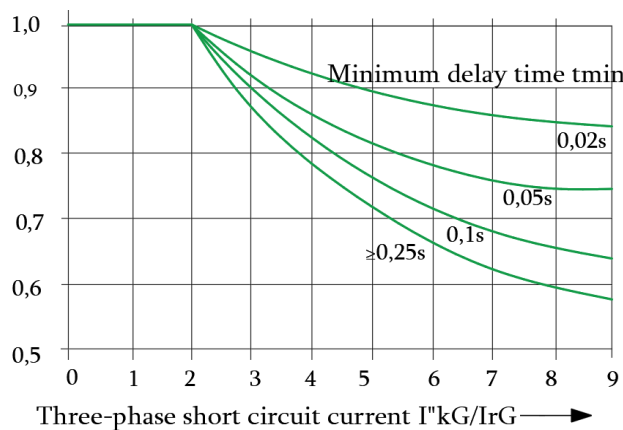


Figure 5. Factor μ for calculating short-circuit breaker current

F. Asymmetric opening current

During the closing or opening of switches, it is necessary to calculate the current flowing at the instant when the contacts separate. Therefore, the asymmetric breaking current must be determined. Starting from the symmetric breaking current I_b of the AC component, and by applying the superposition theorem, the DC component current I_{dc} , evaluated at the same instant, is added [10]. Thus, the breaking current is given by

$$I_{b,asymm} = \sqrt{I_b^2 + I_{dc}^2} \quad (20)$$

where I_{basymm} is the RMS asymmetric breaking current, I_b the RMS symmetric current of the AC component, and I_{dc} the DC component. A more detailed calculation technique involves determining the symmetrical breakdown current while considering the exact opening time, the type of machine, and its proximity to the short-circuit. For this example,

the calculation is performed using a breaking time of 0.1 s, the time defined in the simulations. A detailed report of the results is presented in Table V.

Table V
Breaking and interruption current

Bus	V_{nom} [kV]	ANSI/IEEE			IEC			Relative error [%]
		X/R ratio	M_{Fr}	$I_{adj,symm}$ [kA]	I_{dc}	$I_{b,sym}$	$I_{b,asym}$	
04:MILL-2	13.8	24.832	1.067	13.314	4.049	12.205	12.859	3.42
05:FDR F	13.8	12.844	1	12.897	1.520	12.104	12.199	5.41
10:EMERG	13.8	9.242	1	11.684	0.488	11.603	11.614	0.60
19:T7SEC	2.4	13.265	1	16.661	1.537	17.019	17.088	2.57
50:GEN1	13.8	22.644	1.038	13.528	3.591	12.010	12.535	7.34

Note that, except for the generators, the effective reactances used in IEC are generally lower than those of ANSI/IEEE for short compensation times. Although IEC assumes higher pre-fault voltages, the reactance adjustment becomes the dominant factor, explaining the difference from other comparisons with higher IEC values.

G. ANSI/IEEE's time delay current vs. IEC's steady-state currents

Both the IEC and ANSI/IEEE procedures assume that transient effects have decayed by the time the steady-state current occurs and are therefore not considered in the modeling.

IEC. The amplitude of the permanent short-circuit current I_k depends on the saturation state of the magnetic circuit. For faults located far from the generator, it is computed as follows:

$$I_k = I''_k \quad (21)$$

For faults close to the generator, the maximum and minimum fault currents in the steady state under the highest and lowest excitations of the synchronous generator are given by

$$I_{kmax} = \lambda_{max} \cdot I_{rG} \quad I_{kmin} = \lambda_{min} \cdot I_{rG} \quad (22)$$

where I_{kmax} is the maximum fault current, I_{kmin} the minimum current in the steady state, λ_{max} the maximum scaling coefficient, and λ_{min} the minimum scaling coefficient, which depends on the saturation inductance and the nominal generator current [11]. The values of λ_{max} and λ_{min} are obtained from Fig. 6.

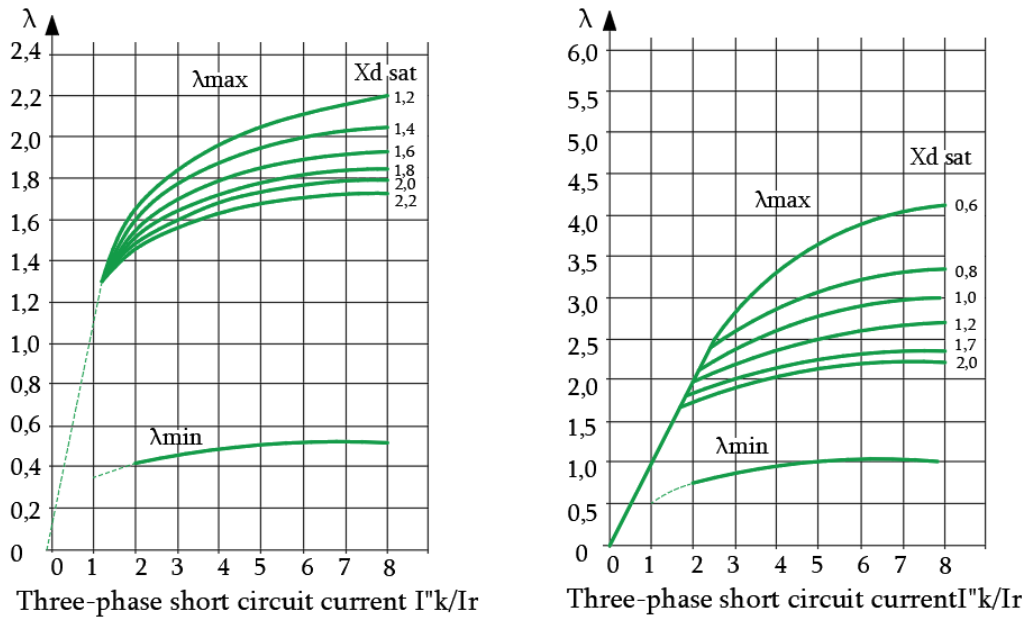


Figure 6. λ_{max} and λ_{min} factors for turbogenerators

ANSI/IEEE. The contributions of all motors are ignored, and only generators contributing to the fault are considered. The DC component is zero in a 30-cycle network. The steady-state reactance of the network components is used to calculate the fault current and the steady-state short-circuit current:

$$I_{est,rms,symm} = \frac{U_f}{\sqrt{3}Z_{eq}} \quad (23)$$

where Z_{eq} denotes the equivalent impedance at the fault point (generators and passive equipment). The permanent and delay short-circuit currents are presented in Table VI.

Table VI
Permanent and delay short-circuit currents

Bus	V_{nom} [kV]	ANSI/IEEE	IEC	Relative error [%]
		$I_{est,rms,symm}$ [kA]	I_k [kA]	
04:MILL-2	13.8	11.455	12.148	6.05
05:FDR F	13.8	11.736	12.089	3.01
10:EMERG	13.8	10.961	11.467	4.61
19:T7SEC	2.4	13.701	14.294	4.33
50:GEN1	13.8	11.921	12.199	2.33

According to ANSI/IEEE standards, the network model includes only generators, which are represented by either their transient reactance or a higher reactance value [5]. ANSI/IEEE uses the transient reactance of the machines. In contrast, IEC assumes that the motors no longer contribute to the short-circuit current. Therefore, the differences between both methods are mainly attributed to the reactance values applied.

VI. CONCLUSIONS

The results reveal significant differences in the short-circuit currents calculated using the IEC and ANSI/IEEE standards, mainly due to their distinct methodological approaches. In general, IEC yields higher short-circuit current values, particularly at buses electrically close to generators. This behavior is consistent with the findings of [4], who emphasize that the IEC standard considers more sustained contributions from rotating machines, leading to more conservative results in complex industrial systems.

Regarding asymmetric closing and blocking currents, the differences between IEC and ANSI/IEEE were below 10%, which supports the equivalence reported in previous studies [1]. This similarity suggests that both standards rely on comparable modeling principles. However, IEC adjusts reactance values according to compensation time, whereas ANSI/IEEE applies transient reactance assumptions. As highlighted by Bandaru [12], this IEC-specific approach becomes particularly relevant in systems where rapid response times are critical.

Regarding the X/R ratio, ANSI/IEEE tends to apply higher reactance multipliers, which generally results in lower calculated short-circuit currents compared to IEC. This discrepancy reinforces the importance of selecting the most appropriate standard based on the characteristics and criticality of the electrical system. While IEC may provide a more conservative perspective that is suitable for highly demanding environments, ANSI/IEEE may be preferable in applications where different assumptions about transient behavior are more representative. The literature consistently indicates that a clear understanding of these methodological differences can support better protection coordination and improve overall system efficiency.

The results confirm the expected behavior in which IEC-based calculations consistently produce higher short-circuit currents than those obtained under ANSI/IEEE criteria. This outcome can be explained by the influence of system topology, particularly the electrical proximity to generation sources and the interconnection paths between buses, as well as by the contribution of rotating machines, whose inertia and transient response are represented differently. These differences are not only relevant from a numerical perspective; they also have direct practical implications for protection coordination, since they affect relay settings, interrupting duties, and equipment withstand capabilities. Consequently, understanding why IEC yields more conservative currents becomes essential for ensuring adequate breaker selection, reliable protection performance, and overall system safety in industrial networks.

This study contributes to a deeper understanding of how IEC and ANSI/IEEE standards influence short-circuit calculations in industrial systems through simulations performed in ETAP 20.0. The accurate modeling of a 44-bus industrial network enabled the evaluation of multiple fault scenarios and a detailed comparison between both regulations. The results also confirmed the high consistency between ETAP simulations and manual calculations, reinforcing the usefulness of software tools in system planning and protection design. Nevertheless, since the analysis was limited to a single industrial configuration, future work should extend the comparison to different voltage levels, network topologies, and additional international standards, including scenarios with emerging generation and storage technologies.

AVAILABILITY OF DATA AND MATERIALS

The data presented in this study are available from the corresponding author upon request.

FUNDING

This research received no external funding.

CREDIT AUTHOR CONTRIBUTION STATEMENT

J. Muñoz-Goez: conceptualization, methodology, validation, writing (review and editing).
J. Sosapanta-Salas: methodology, research, formal analysis, writing (review and editing).
J. Noguera-Jiménez: supervision, conceptualization, methodology, validation, writing (original draft, review, and editing).

DECLARATION OF COMPETING INTEREST

The authors declare that they have no known competing financial interests or personal relationships that could appear to have influenced the study reported in this paper.

USE OF ARTIFICIAL INTELLIGENCE (AI)

During this work, the authors did not employ any technologies associated with artificial intelligence.

REFERENCES

- [1] I. C. Choachi Gómez and Á. J. López Loaiza, “Estudio comparativo de las normas IEC 60909-0 y ANSI/IEEE 141-4 para el cálculo de corrientes de cortocircuito en instalaciones eléctricas de uso final empleando los simuladores Digsilent PowerFactory y ETAP,” Undergraduate thesis, Univ. Tecnológica de Pereira, Pereira, Colombia, 2017. [Online]. Available: <https://hdl.handle.net/11059/8426>
- [2] IEEE Power and Energy Society, “IEEE application guide for AC high-voltage circuit breakers >1000 Vac rated on a symmetrical current basis,” *IEEE Std C37.010-2016*, 2016. <https://doi.org/10.1109/IEEESTD.2017.7906465>
- [3] International Electrotechnical Commission, “Short-circuit currents in three-phase a.c. systems – Part 0: Calculation of currents,” *IEC 60909-0*, 2016. [Online]. Available: <https://webstore.iec.ch/en/publication/24100>
- [4] R. Chelluri and M. D. Mohapatra, “Comparison of ANSI–IEC short circuit methods,” *Int. J. Adv. Res. Electr. Electron. Instrum. Eng.*, vol. 8, no. 9, pp. 2182–2188, Sep. 2019. <https://doi.org/10.1109/28.297928>

- [5] S. J. Muñoz Goez and P. Mesa Beleño, “Análisis comparativo de las normas ANSI/IEEE Std C37.010-2016, IEEE Std C37.13-2015, IEEE Std C37.5-1979, IEEE Std 141-1993 and IEC 60909-2016 para el cálculo de corrientes de cortocircuito,” Undergraduate thesis, Institución Universitaria Pascual Bravo, Medellín, Colombia, 2024.. <https://repositorio.pascualbravo.edu.co/handle/pascualbravo/2536>
- [6] J. Catagua and A. Valdivieso, “Análisis de cortocircuito en un sistema industrial bajo normativas ANSI e IEC, simulados en Digsilent PowerFactory,” Undergraduate thesis, Univ. Politécnica Salesiana, Ecuador, 2024. [Online]. Available: <http://dspace.ups.edu.ec/handle/123456789/28685>
- [7] J. C. Das, *Power system analysis: Short-circuit load flow and harmonics*, 2nd ed. Boca Raton, FL, USA: CRC Press, 2017. <https://doi.org/10.1201/b11021>
- [8] H. Arboleda, “Aplicación del análisis de flujos de carga y cortocircuito a la optimización del diseño de un sistema eléctrico industrial,” Undergraduate thesis, Univ. del Valle, Cali, Colombia, 2017. <https://hdl.handle.net/20.500.14330/TES01000759661>
- [9] M. Brenna and Y. A. M. Mohammed, “Short-circuit fault level calculation on 33/11 kV substation by using ETAP simulator according to the IEC 60909 standard,” MS thesis, Politec. di Milano, Milan, Italy, 2020. <https://www.politesi.polimi.it/handle/10589/166274>
- [10] IEEE, “IEEE recommended practice for conducting short-circuit studies and analysis of industrial and commercial power systems,” *IEEE Std 3002.3-2018*, 2019. <https://doi.org/10.1109/IEEESTD.2019.8672198>
- [11] R. Luo, A. Majd, and M. Devadass, “Comprehensive overview and comparisons of ANSI vs. IEC short-circuit calculations,” presented at 2018 *IEEE Petrol. Chem. Ind. Tech. Conf. (PCIC)*, 2019. <https://doi.org/10.1109/PCIC31437.2018.9080479>
- [12] D. Bandaru, S. R. Sura, J. K. Bokam, and K. A. Kumar, “Methods for Short Circuit Analysis in ANSI and IEC Standards,” *Int. J. Mech. Eng.*, vol. 7, no. 2, 5487–5493, 2022. <https://doi.org/10.1109/TIA.2019.2919479>
- [13] D. Brankovic and R. Schuerhuber, “Short-circuit current of a hydropower plant with consideration of constant switching and fault arc voltages,” *IET Gener., Transm. Distrib.*, vol. 18, pp. 3476-3486, 2024. <https://doi.org/10.1049/gtd2.13297>
- [14] A. Heyduk and J. Joostberens, “Comparative analysis of European and American standards for maximum fault current calculations on medium voltage mine power networks,” *Elektron. Elektrotech.*, vol. 22, no. 2, pp. 13–20, 2016. <https://doi.org/10.5755/j01.eie.22.2.14608>
- [15] S. N. Afifi and M. Darwish, “Impact of hybrid distributed generation allocation on short circuit currents in distribution systems,” PhD dissertation, Brunel Univ., London, UK, 2017. <https://doi.org/10.1109/UPEC.2014.6934697>
- [16] P. A. Salvatierra Villavicencio, “Simulación de una red soterrada de distribución de energía eléctrica de potencia bajo la norma IEC 60909/ANSI,” Master’s thesis, Universidad Politécnica Salesiana, Ecuador, 2021. [Online]. Available: <http://dspace.ups.edu.ec/handle/123456789/20185>

- [17] Y. N. Lafta, N. A. Shalash, Y. N. Abd, and A. A. Al-Lami, "IEC 60909 and ANSI standards comparison with ASCC-based fault calculations of Iraqi power system," *Cogent Eng.*, vol. 6, no. 1, Art. no. 1559545, Jan. 2019. <https://doi.org/10.1080/23311916.2019.1705654>
- [18] B. Niersbach, I. Ghourabi, B. Braun, and J. Hanson, "Advanced modelling of inverter-based generators for short-circuit current calculations based on IEC 60909-0:2016," in *Proc. IEEE PowerTech*, Milan, Italy, 2019, pp. 1–6. <http://dx.doi.org/10.34890/837>
- [19] H. Peláez Velásquez, "Análisis comparativo de las fallas simétricas aplicando las normas ANSI/IEEE C37.10 e IEC 60909 con el paquete computacional NEPLAN," Undergraduate thesis, Universidad Tecnológica de Pereira, Pereira, Colombia, 2015. [Online]. Available: <https://hdl.handle.net/11059/6033>
- [20] O. Álvarez Lastra, "Simulación de cortocircuitos en sistemas eléctricos de potencia usando métodos tradicionales y normativas," Undergraduate thesis, Univ. Politécnica Salesiana, 2020. <https://dspace.ups.edu.ec/handle/123456789/19339>
- [21] W. D. Mendoza Pardo and J. P. Samaniego Avalos, "Validación del programa ATP para estudios de cortocircuitos en sistemas eléctricos de potencia," Undergraduate thesis, Universidad Politécnica Salesiana, Ecuador, Apr. 2023. [Online]. Available: <http://dspace.ups.edu.ec/handle/123456789/24681>
- [22] Y. Zhang *et al.*, "The adaptability of IEC 60909-0-2016 to power grid with voltage levels above 400 kV," *J. Phys. Conf. Ser.*, vol. 2276, no. 1, art. 012018, May 2022. <https://doi.org/10.1088/1742-6596/2276/1/012018>
- [23] J. C. Barrantes Quesada, "Estudio de cortocircuito y coordinación de protecciones en CVG ALUNASA," *undergraduate thesis*, Universidad de Costa Rica, San José, Costa Rica, 2014. <https://ruie.ucr.ac.cr/catalogo/Record/INII-UJR-CD-13557>
- [24] V. J. V. Bojórquez, "Estudio comparativo de las normas IEC y ANSI para cálculo de corto circuito," Master's thesis, Instituto Politécnico Nacional, Escuela Superior de Ingeniería Mecánica y Eléctrica, México, D.F., México, Sept. 2007. [Online]. Available: <https://www.zlibrary.to/dl/estudio-comparativo-de-las-normas-iec-y-ansi-para-calculo-de-corto-circuito>
- [25] S. Lakshmi Sankar and M. Mohamed Iqbal, "ANSI and IEC standards based short circuit analysis of a typical 2 × 30 MW thermal power plant," *Middle-East J. Sci. Res.*, vol. 23, no. 8, pp. 1617–1625, 2015.
- [26] D. Schulz, Ed., *Proceedings of the NEIS 2020 Conference on Sustainable Energy Supply and Energy Storage Systems*. Berlin, Germany: VDE Verlag, 2020. [Online]. Available: <https://www.researchgate.net/publication/361927719>